Design, Synthesis, and Biochemical Evaluation of 1,5,6,7-Tetrahydro-6,7-dioxo-9-D-Ribitylaminolumazines Bearing Alkyl Phosphate Substituents as Inhibitors of Lumazine Synthase and Riboflavin Synthase

Mark Cushman,*,† Guangyi Jin,† Boris Illarionov,‡ Markus Fischer,‡ Rudolf Ladenstein,§ and Adelbert Bacher‡

Department of Medicinal Chemistry and Molecular Pharmacology and the Purdue Cancer Center, School of Pharmacy and Pharmaceutical Sciences, Purdue University, West Lafayette, Indiana 47907, Lehrstuhl für Organische Chemie und Biochemie, Technische Universität München, D-85747 Garching, Germany, and NOVUM Centre for Structural Biochemistry, Karolinska Institute, S-14157 Huddinge, Sweden

cushman@pharmacy.purdue.edu
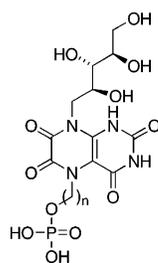
Inhibition Constants vs. *Mycobacterium tuberculosis* Lumazine Synthase		
n	K_i	mechanism
4	36 ± 4 nM	competitive
5	12 ± 4 nM	competitive

The last two steps in the biosynthesis of riboflavin, an essential metabolite that is involved in electron transport, are catalyzed by lumazine synthase and riboflavin synthase. To obtain structural probes and inhibitors of these two enzymes, two ribityllumazinediones bearing alkyl phosphate substituents were synthesized. The synthesis involved the generation of the ribityl side chain, the phosphate side chain, and the lumazine system in protected form, followed by the simultaneous removal of three different types of protecting groups. The products were designed as intermediate analogue inhibitors of lumazine synthase that would bind to its phosphate-binding site as well as its lumazine binding site. Both compounds were found to be effective inhibitors of *Bacillus subtilis* lumazine synthase as well as *Escherichia coli* riboflavin synthase. Molecular modeling of the binding of one of the two compounds provided a structural explanation for how these compounds are able to effectively inhibit both enzymes. In phosphate-free buffer, the phosphate moieties of the inhibitors were found to contribute positively to their binding to *Mycobacterium tuberculosis* lumazine synthase, resulting in very potent inhibitors with K_i values in the low nanomolar range. The additional carbonyl in the dioxolumazine system versus the purinetrione system was found to make a positive contribution to its binding to *E. coli* riboflavin synthase.

Introduction

The last two steps in the biosynthesis of riboflavin (Scheme 1) involve the lumazine synthase-catalyzed reaction of the four-carbon phosphate **2** with the ribityl-laminopyrimidinedione **1** to form 6,7-dimethyl-8-ribityl-lumazine (**3**), followed by the riboflavin synthase-catalyzed dismutation of two molecules of **3** to form one molecule of riboflavin (**4**) and one molecule of the lu-

mazine synthase substrate **1**. In a beautiful example of natural recycling, the product **1** of the riboflavin synthase-catalyzed reaction is then utilized by lumazine synthase. The overall stoichiometry involves the consumption of one molecule of the pyrimidinedione **1** and two molecules of the organophosphate **2** to form one molecule of riboflavin (**4**).[1-5]

* Corresponding author: phone 765-494-1465, fax 765-494-6790.
† Purdue University.
‡ Technische Universität München.
§ Karolinska Institute.

(1) Plaut, G. W. E.; Smith, C. M.; Alworth, W. L. *Annu. Rev. Biochem.* **1974**, *43*, 899−922.
(2) Plaut, G. W. E. In *Comprehensive Biochemistry*; Florkin, M., Stotz, E. H., Eds.; Elsevier: Amsterdam, 1971; Vol. 21, pp 11−45.
(3) Beach, R. L.; Plaut, G. W. E. *J. Am. Chem. Soc.* **1970**, *92*, 2913−2916.
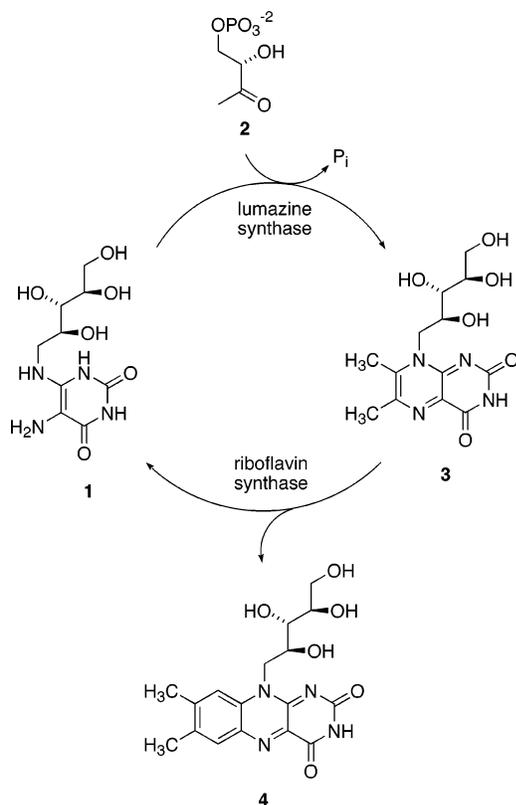
SCHEME 1

SCHEME 2

The mechanism proposed for the lumazine synthase-catalyzed reaction has gone through several iterations, the most recent of which is outlined in Scheme 2.[6] The location of the phosphate moiety in the enzyme complex involving the hypothetical intermediate **5**, relative to the remainder of the molecule, is roughly approximated as shown in the structure of the initial carbinolamine intermediate **5** as displayed in Scheme 2, as evidenced by the crystal structure of the complex formed between *Saccharomyces cerevisiae* lumazine synthase and the intermediate analogue **11**[7] (Figure 1).[8] Rotation of the whole phosphate-containing side chain toward the ribitylamino moiety would then generate conformer **6**, which could eliminate water to form the cis Schiff base **7**. Phosphate elimination would lead to the enol **8**, followed by tautomerization to the ketone **9**. Nucleophilic attack of the ribitylamino group on the ketone would result in the carbinolamine **10**, which could eliminate water to form the final product **3**.
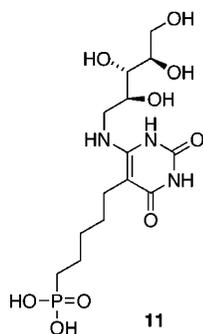
Although the pathway outlined in Scheme 2 seems reasonable from a structural and mechanistic point of
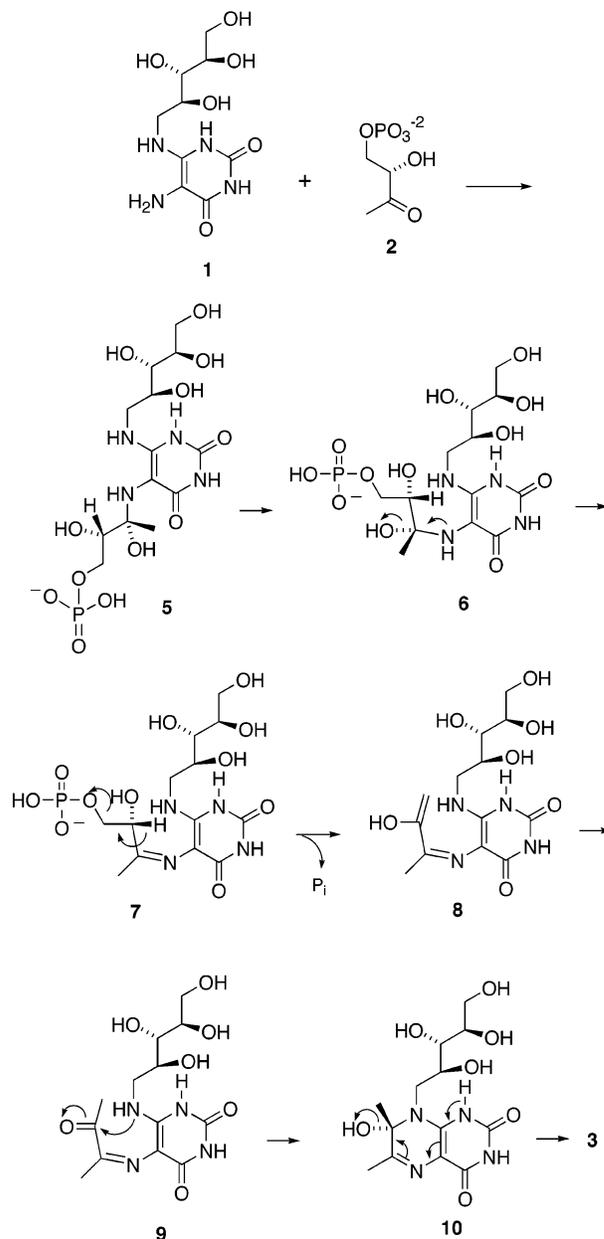
view, the exact sequence of the events required to form the final product has not been rigorously established. For example, phosphate elimination could occur after Schiff base formation and before the conformational reorganization of the side chain to favor formation of the six-membered ring.[9]

When determined in the presence of fixed substrate **1** concentration and variable substrate **2** concentration, the

(4) Bacher, A.; Eberhardt, S.; Richter, G. In *Escherichia coli and Salmonella: Cellular and Molecular Biology*; 2nd ed.; Neidhardt, F. C., Ed.; ASM Press: Washington, D. C., 1996; p 657−664.

(5) Bacher, A.; Fischer, M.; Kis, K.; Kugelbrey, K.; Mörtl, S.; Scheuring, J.; Weinkauf, S.; Eberhardt, S.; Schmidt-Bäse, K.; Huber, R.; Ritsert, K.; Cushman, M.; Ladenstein, R. *Biochem. Soc. Trans.* **1996**, *24*, 89−94.

(6) Zhang, X.; Meining, W.; Cushman, M.; Haase, I.; Fischer, M.; Bacher, A.; Ladenstein, R. *J. Mol. Biol.* **2003**, *328*, 167−182.

(7) Cushman, M.; Mihalic, J. T.; Kis, K.; Bacher, A. *J. Org. Chem.* **1999**, *64*, 3838−3845.

(8) Meining, W.; Mörtl, S.; Fischer, M.; Cushman, M.; Bacher, A.; Ladenstein, R. *J. Mol. Biol.* **2000**, *299*, 181−197.

(9) Volk, R.; Bacher, A. *J. Am. Chem. Soc.* **1988**, *110*, 3651−3653.
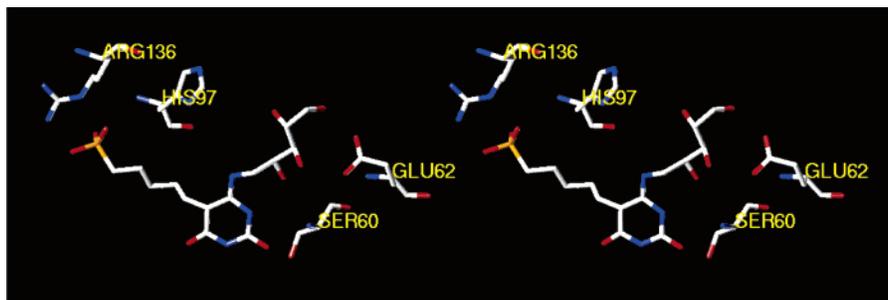
FIGURE 1. Crystal structure of phosphonate **11** bound in the active site of *S. cerevisiae* lumazine synthase.[8] The figure is programmed for walleyed viewing.

phosphonate **11** is a moderately active inhibitor of *Bacillus subtilis* lumazine synthase (mixed inhibition, K_i 180 μM, K_{is} 350 μM).[7] When tested under the same conditions, the purinetrione **12** proved to be more potent, displaying mixed inhibition with a K_i of 46 μM and a K_{is} of 250 μM.[10] The combination of the purinetrione ring system with a C-5 phosphate side chain to form **13** resulted in a less potent inhibitor of *B. subtilis* lumazine synthase (K_i 852 μM, K_{is} 817 μM) when tested in the presence of variable substrate **2** concentration.[11] However, the substituted purinetrione **13** unexpectedly proved to be a very potent competitive inhibitor of *Mycobacterium tuberculosis* lumazine synthase when tested in Tris buffer (phosphate-free) with a K_i of 4.7 nM![11] The selectivity of this compound and its phosphate homologues for the *M. tuberculosis* enzyme as opposed to the *B. subtilis* enzyme is truly remarkable. The alkylphosphonate side chain does in fact contribute positively to inhibition of *M. tuberculosis* lumazine synthase, since the purinetrione system **12** itself is a K_i 9.1 μM inhibitor of the enzyme.[11] The alkylphosphonate derivative **13** is also a competitive inhibitor of *Escherichia coli* riboflavin synthase with a K_i of 2.44 μM.[11]
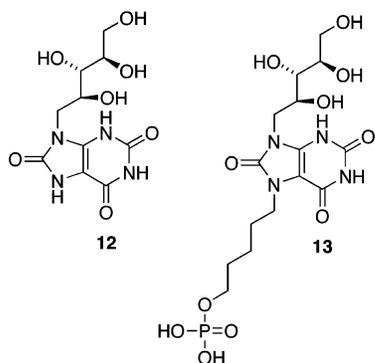
These results suggest consideration of the 6,7-dihydro-6,7-dioxo-8-ribityllumazine system **14**, which was previously shown to be an exceedingly potent inhibitor of baker's yeast riboflavin synthase (K_i 25 nM)[12] and *Ashbya gossypii* riboflavin synthase (K_i 9 nM).[13] This led to the

hypothesis that the attachment of alkyl phosphate side chains on N-5 of the 6,7-dioxo-8-ribityllumazine (**14**) system would likely result in promising inhibitors of *E. coli* riboflavin synthase as well as *M. tuberculosis* lumazine synthase. The present paper describes the synthesis and biological testing of the suggested five-carbon and six-carbon alkyl phosphate derivatives of **14**.

14
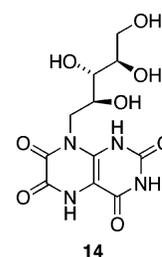
The rationale for the potential medical use of riboflavin synthase inhibitors stems from the fact that certain Gram-negative pathogenic bacteria and yeasts have been shown to lack an efficient riboflavin uptake system and are therefore absolutely dependent on endogenous riboflavin biosynthesis.[14–17] In contrast, humans lack riboflavin biosynthesis enzymes and obtain this essential nutrient entirely from dietary sources. Therefore, inhibitors of riboflavin biosynthesis can be expected to display selective cytotoxicity for pathogenic microorganisms as opposed to human cells.

Results and Discussion

The linker from the phosphate to the pyrimidine ring in the proposed reaction intermediate **5** is four atoms long, and the results from previous studies on the purinetrione derivative **13** and its homologues revealed that the best linkers between phosphate and purinetrione ring are from three to five atoms long for inhibition of *M. tuberculosis* lumazine synthase. It was therefore logical to choose the alkyl phosphate derivatives of **14** with polymethylene chains containing four and five carbon atoms.[11,18]

(10) Cushman, M.; Yang, D.; Kis, K.; Bacher, A. *J. Org. Chem.* **2001**, *66*, 8320–8327.

(11) Cushman, M.; Sambaiah, T.; Jin, G.; Illarionov, B.; Fischer, M.; Bacher, A. *J. Org. Chem.* **2004**, *69*, 601–612.

(12) Al-Hassan, S. S.; Kulick, R. J.; Livingston, D. B.; Suckling, C. J.; Wood, H. C. S.; Wrigglesworth, R.; Ferone, R. *J. Chem. Soc., Perkin Trans. 1* **1980**, 2645–2656.

(13) Winestock, C. H.; Aogaichi, T.; Plaut, G. W. E. *J. Biol. Chem.* **1963**, *238*, 2866–2874.

(14) Wang, A. *I Chuan Hsueh Pao* **1992**, *19*, 362–368.

(15) Oltmanns, O.; Lingens, F. *Z. Naturforsch., B: Anorg. Chem., Org. Chem., Biochem., Biophys., Biol.* **1967**, *22b*, 751–754.

(16) Logvinenko, E. M.; Shavlovsky, G. M. *Mikrobiologiya* **1967**, *41*, 978–979.

(17) Neuberger, G.; Bacher, A. *Biochem. Biophys. Res. Commun.* **1985**, *127*, 175–181.

(18) Morgunova, K.; Meining, W.; Illarionov, B.; Haase, I.; Jin, G.; Bacher, A.; Cushman, M.; Fischer, M.; Ladenstein, R. *Biochemistry* **2005**, *44*, 2746–2758.

SCHEME 3[a]

[Chemical scheme showing structures 15, 16 (36%), 17 n = 4 (63%), 18 n = 5 (68%), 19 n = 4 (70%), 20 n = 5 (71%), 21 n = 4 (73%), 22 n = 5 (78%), with reagents a, b, c, d]
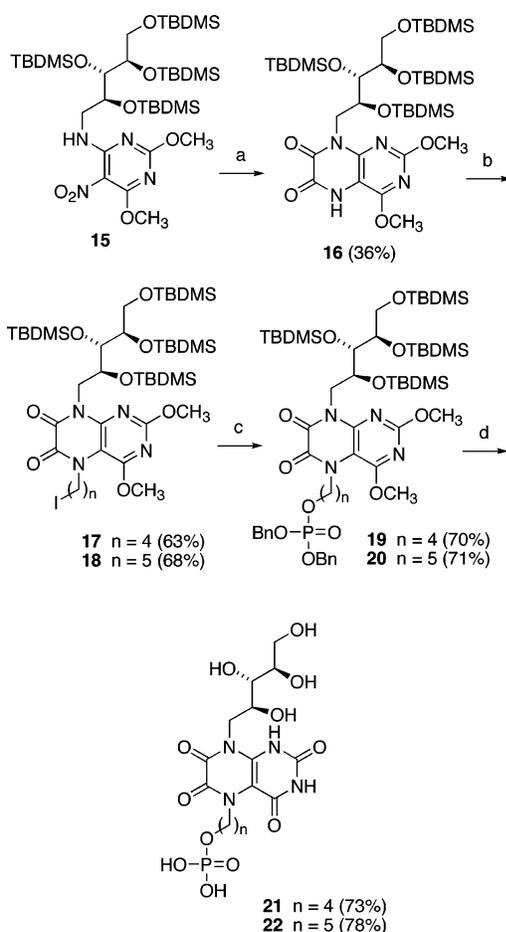
[a] Reagents and conditions: (a) (1) H_2, Pd/C, MeOH, 23 °C (3 days); (2) EtOCOCOCl, Et$_3$N, CH$_2$Cl$_2$, 0 °C (10 h); (3) Et$_3$N, EtOH, reflux (72 h). (b) Diiodoalkane, K$_2$CO$_3$, CH$_3$CN, reflux (10 h). (c) AgOPO(OBn)$_2$, CH$_3$CN, reflux (12 h). (d) [48% HBr−H$_2$O (2:1)]−MeOH (1:1), 55−60 °C (3 h).

The syntheses of the two phosphates **21** and **22** having four- and five-methylene linker chains between the phosphate and the lumazinedione ring system are outlined in Scheme 3. Since the lumazinedione ring system **14** and the ribityl hydroxyl groups can be alkylated, the synthesis required the generation of these two moieties in protected form before the desired alkylation reaction could be carried out. Starting from the known pyrimidine **15**,[11] catalytic reduction of the nitro group over palladium on carbon yielded an unstable amine intermediate that was reacted immediately with ethyl chlorooxoacetate, followed by heating the intermediate with triethylamine in refluxing ethanol, to provide the pteridine system **16**. Reaction of **16** with 1,4-diiodobutane and 1,5-diiodopentane resulted in displacement of one of the iodides from each diiodo compound to afford the desired alkyl iodides **17** and **18**. Displacement reactions on the iodides **17** and **18** with silver dibenzyl phosphate resulted in the alkyl phosphates **19** and **20**. Simultaneous removal of all three types of protecting groups (TBDMS, methyl, and benzyl) was accomplished by heating intermediates **19** and **20** with HBr in aqueous methanol at 55−60 °C to afford the target compounds **21** and **22** in good yields.

The phosphates **21** and **22** were tested as inhibitors of recombinant *B. subtilis* lumazine synthase β_{60} capsids,

TABLE 1. Inhibition Constants versus *B. subtilis* Lumazine Synthase, *M. tuberculosis* Lumazine Synthase, and *E. coli* Riboflavin Synthase

parameter	lumazine synthase		riboflavin synthase
	B. subtilis[a]	*M. tuberculosis*[b]	*E. coli*[c]
Compound 14			
inhibition mechanism	competitive	competitive	competitive
K_s^d (μM)	6.3 ± 0.5	250 ± 43	2.7 ± 0.2
k_{cat}^e (min^{-1})	2.6 ± 0.1	1.1 ± 0.1	15.0 ± 0.3
K_i^f (μM)	7.8 ± 0.5	1.4 ± 0.1	**0.0062 ± 0.0005**
Compound 21			
inhibition mechanism	mixed	competitive	mixed
K_s (μM)	7.1 ± 1.0	240 ± 29	2.5 ± 0.3
k_{cat} (min^{-1})	2.1 ± 0.1	1.2 ± 0.1	15.0 ± 0.4
K_i (μM)	150 ± 43	**0.036 ± 0.004**	9.7 ± 4.1
K_{is}^g (μM)	400 ± 130		21 ± 5
Compound 22			
inhibition mechanism	competitive	competitive	competitive
K_s (μM)	5.8 ± 0.4	210 ± 28	2.9 ± 0.4
k_{cat} (min^{-1})	2.7 ± 0.1	0.99 ± 0.07	14 ± 1
K_i (μM)	27 ± 6	**0.012 ± 0.004**	**0.14 ± 0.02**
Compound 23			
inhibition mechanism	competitive	competitive	competitive
K_s (μM)	3.2 ± 0.4	63 ± 6	2.1 ± 0.2
k_{cat} (min^{-1})	3.1 ± 0.1	1.4 ± 0.1	17.0 ± 0.4
K_i (μM)	170 ± 26	**0.0041 ± 0.0023**	330 ± 83
Compound 24			
inhibition mechanism	mixed	competitive	competitive
K_s (μM)	3.8 ± 0.4	63 ± 5	2.0 ± 0.2
k_{cat} (min^{-1})	3.15 ± 0.10	1.40 ± 0.04	17.0 ± 0.4
K_i (μM)	270 ± 85	**0.0047 ± 0.0019**	2.4 ± 0.2
K_{is} (μM)	650 ± 160		

[a] Recombinant lumazine synthase from *B. subtilis*. [b] Recombinant lumazine synthase from *M. tuberculosis*. [c] Recombinant riboflavin synthase from *E. coli*. [d] K_s is the substrate dissociation constant for the equilibrium E + S $\rightleftharpoons$ ES. [e] k_{cat} is the rate constant for the process ES → E + P. [f] K_i is the inhibitor dissociation constant for the process E + I $\rightleftharpoons$ EI. [g] K_{is} is the inhibitor dissociation constant for the process ES + I $\rightleftharpoons$ ESI. K_i values of less than 1 μM are shown in boldface type.

recombinant *E. coli* riboflavin synthase, and recombinant *M. tuberculosis* lumazine synthase. The inhibition constants and inhibition mechanisms for **21** and **22** are listed in Table 1. To evaluate the effect of substitution with the alkyl phosphate chains in these compounds, the dioxolumazine system **14** itself was also tested as an inhibitor of all three enzymes, and the previously determined data for the purinetriones **23** and **24** are also listed in Table 1 for comparison.[11] Representative Lineweaver−Burk plots for inhibition of *B. subtilis* lumazine synthase, *M. tuberculosis* lumazine synthase, and *E. coli* riboflavin synthase by inhibitor **22** are presented in Figure 2.

[Chemical structures 23 n = 4, 24 n = 5]
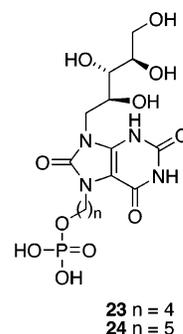
Crystal structures are now available for complexes formed between the substrate analogue **25** and the
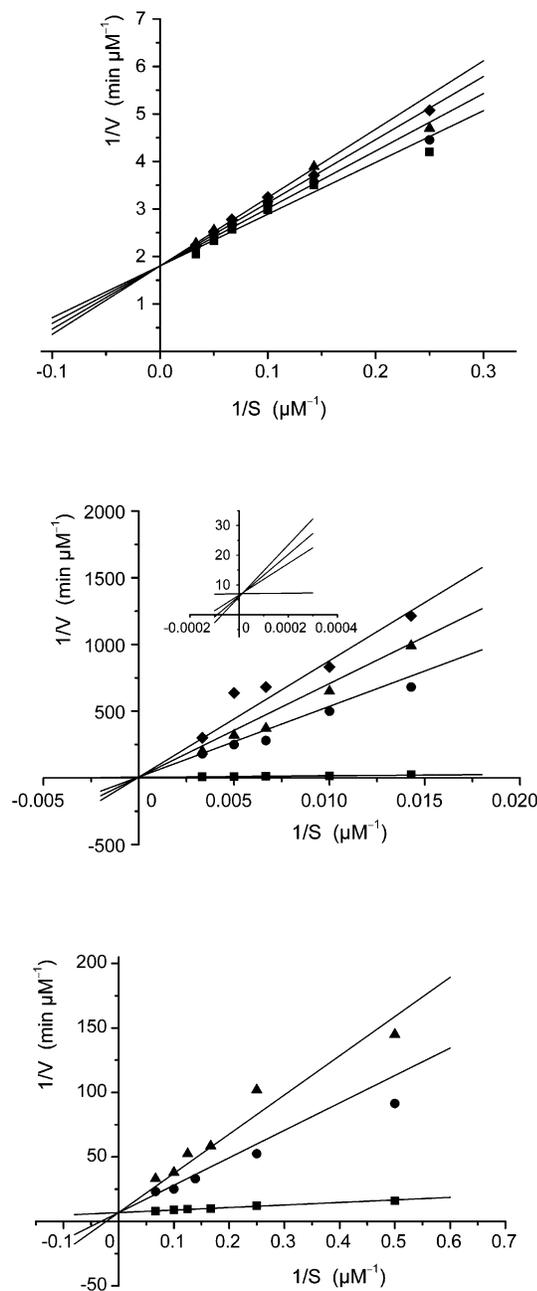
FIGURE 2. Lineweaver–Burk plots for the inhibition of *B. subtilis* lumazine synthase by inhibitor **22** (top panel; inhibitor concentrations 0, 3.0, 6.0, and 8.6 μM, mechanism competitive), *M. tuberculosis* lumazine synthase (center panel; inhibitor concentrations 0, 0.8, 1.0, and 1.2 μM, mechanism competitive), and *E. coli* riboflavin synthase (bottom panel; inhibitor concentrations 0, 1.5, and 2.0 μM, mechanism competitive). The inset in the middle panel shows an expanded view of the simulation plot in the region $1/S = 0$. The kinetic data were fitted with a nonlinear regression method by the program Dynafit.[25] Different kinetic models were considered, and the most likely inhibition mechanism was determined to be competitive inhibition in each case.

lumazine synthases of *B. subtilis* and *Schizosaccharomyces pombe*.[19,20] The X-ray structures of the intermediate analogue **11** bound to *S. cerevisiae* lumazine synthase (Figure 1),[8] the product analogue **26** bound to *S. pombe* lumazine synthase,[20] and the intermediate analogue inhibitor **23** and its lower homologue bound to *M.*

tuberculosis lumazine synthase all allow the rational docking and energy minimization of additional lumazine synthase inhibitors to create hypothetical structures of their enzyme complexes. In the present case, a molecular model was constructed by overlapping the structure of **22** with that of **25** in a 15 Å spherical fragment surrounding the ligand in one of the 60 equivalent active sites of *B. subtilis* lumazine synthase. The structure of **25** was then deleted and the energy of the complex was minimized by use of the MMFF94s force field and MMFF94 charges, while the ligand and the protein structure contained within a 6 Å sphere surrounding the ligand were allowed to be flexible and the remainder of the protein structure was immobile. The resulting structure is displayed in Figure 3, which shows the bound ligand **22** (red) and the surrounding amino acid residues of the protein that are calculated to be involved in hydrogen bonding (yellow lines) to the ligand. The calculated structure of the complex shows the expected stacking of the lumazinedione ring system of the ligand with the benzene ring of Phe22. There is extensive bonding of the phosphate moiety with the side-chain nitrogens of Arg127, the side-chain hydroxyl of Thr86, and the backbone nitrogens of Thr86 and Ala85. The imide fragment of the heterocyclic system has contacts with the backbone nitrogen of Ala56, the backbone carbonyl of Thr80, and the side-chain nitrogen of Asn23. The side-chain nitrogen of Lys135 is calculated to play a strong role in stabilizing the complex, with possible hydrogen-bonding contacts with the C-7 carbonyl of the heterocyclic system of the ligand as well as with the 3′- and 4′-hydroxyl groups. A water molecule hydrogen-bonds to the 2′-hydroxyl group of the ribityl moiety, and the 4′-hydroxyl group hydrogen-bonds to the side-chain carbonyl of Phe113′. The 5′-hydroxyl group is calculated to bond to the side-chain hydroxy group of Ser142 and the carboxyl of Glu58. All of the calculated hydrogen bonds and distances are displayed in Figure 4.
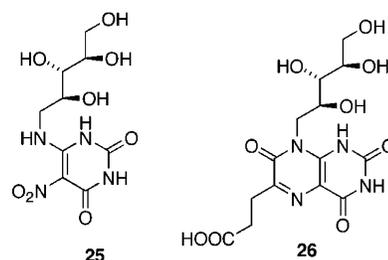
New antibiotics that are active against drug-resistant *M. tuberculosis* are needed urgently. Therefore, the phosphates **21** and **22**, as well as the parent compound **14**, were tested as inhibitors of *M. tuberculosis* lumazine synthase. Both of the phosphates **21** (K_i 0.036 μM) and **22** (K_i 0.012 μM), like **23** and **24**, proved to be very potent inhibitors with K_i values in the low nanomolar range. Interestingly, the attachment of the phosphate chains to the lumazinedione **14** caused a dramatic increase in potency versus *M. tuberculosis* lumazine synthase (com-

(19) Ritsert, K.; Huber, R.; Turk, D.; Ladenstein, R.; Schmidt-Bäse, K.; Bacher, A. *J. Mol. Biol.* **1995**, *253*, 151–167.
(20) Gerhardt, S.; Haase, I.; Steinbacher, S.; Kaiser, J. T.; Cushman, M.; Bacher, A.; Huber, R.; Fischer, M. *J. Mol. Biol.* **2002**, *318*, 1317–1329.
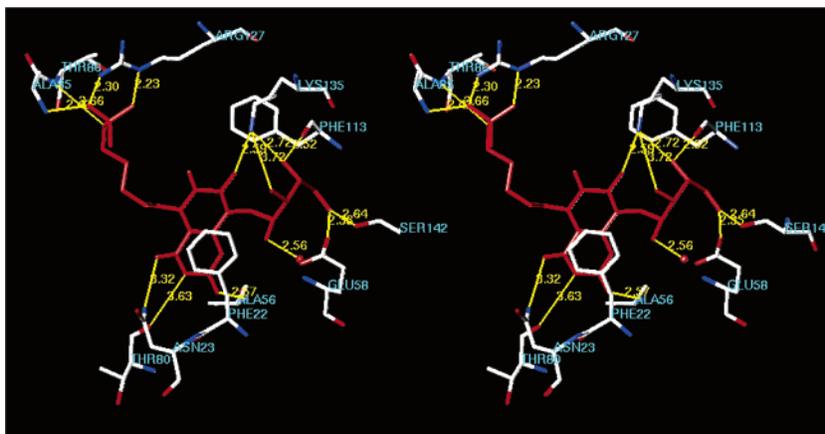
FIGURE 3. Hypothetical model for the binding of compound **22** to *B. subtilis* lumazine synthase. The figure is programmed for walleyed viewing.
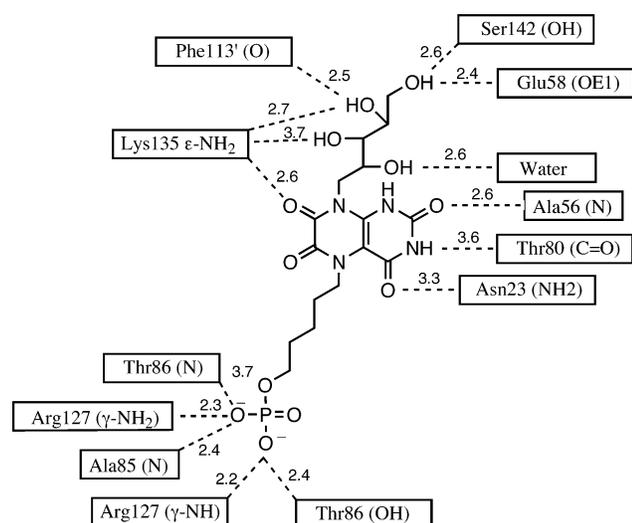
FIGURE 4. Hydrogen bonds and distances in the calculated model of the inhibitor **22** bound in the active site of *B. subtilis* lumazine synthase.

pare **14** versus **21** and **22**). This is in contrast to the results seen with the *B. subtilis* enzyme, where decreases in potency resulted from side-chain attachment when tested in the presence of variable substrate **1** concentration. As with the *B. subtilis* enzyme, the increase in the side-chain length resulted in a modest increase in potency versus *M. tuberculosis* lumazine synthase (compare **21** versus **22**). However, both **21** and **22** appeared to be slightly less active versus *M. tuberculosis* lumazine synthase than **23** and **24**. All of the compounds tested proved to be competitive inhibitors of *M. tuberculosis* lumazine synthase.

The purinetrione system **12** can be considered to be a product analogue of lumazine synthase and a substrate analogue of riboflavin synthase. Accordingly, it was previously tested as an inhibitor of both enzymes and found to be a K_i 46 μM inhibitor of *B. subtilis* lumazine synthase (with variable **2** concentration) and a 0.61 μM inhibitor of *E. coli* riboflavin synthase.[10] However, unexpectedly, the phosphate derivatives **23** and **24** also proved to be riboflavin synthase inhibitors.[11] Accordingly, both lumazindione derivatives **21** and **22** were tested versus *E. coli* riboflavin synthase. Compound **21** was a

mixed inhibitor with K_i 9.7 μM and K_{is} 21 μM, while **22** was a competitive inhibitor with K_i 0.14 μM. This documents a significant effect of chain length on potency, and it is similar to the effect seen with the purinetriones **23** and **24**. However, both of the lumazinedione phosphate derivatives **21** and **22** were much less active than the lumazinedione system **14** itself (K_i 0.0062 μM), so the attachment of the phosphate side chains to these molecules causes a significant drop in potency versus *E. coli* riboflavin synthase. One of the reasons for originally conducting this study was to test the hypothesis that the pyrimidinediones **21** and **22** would be more potent as riboflavin synthase inhibitors than the purinetriones **23** and **24**, and the results indicate that they in fact are more potent inhibitors. The additional carbonyl group present in **21** and **22** therefore does have a significantly positive effect on the riboflavin synthase enzyme inhibitory activity that is also reflected in the parent compounds **12** (K_i 0.61 μM) and **14** (K_i 0.0062 μM).

The crystal structure of *E. coli* riboflavin synthase, which contains three identical subunits, has been published along with a hypothetical model of bound substrate **3**.[21] A crystal structure has also been determined of monomeric *S. pombe* riboflavin synthase with bound substrate analogue **26**,[22] and an NMR investigation of the structure of the N-terminal domain of riboflavin synthase has also appeared.[23] The studies have established that the active site of riboflavin synthase is derived from the intermolecular juxtaposition of residues belonging to both of the barrels in the C-terminal and N-terminal domains of two subunits, with one substrate molecule bound to each barrel. Thus, structures are available for the trimeric apoenzyme and a ligand-bound monomer, and the structures of the active site can be proposed by combining elements of the two structures. The structures allow the molecular modeling of the complex formed between *E. coli* riboflavin synthase and the inhibitor **22** by a similar procedure as described for

(21) Liao, D.-I.; Wawrzak, Z.; Calabrese, J. C.; Viitanen, P. V.; Jordan, D. B. *Structure* **2001**, *9*, 399−408.
(22) Gerhardt, S.; Schott, A.-K.; Kairies, N.; Cushman, M.; Illarionov, B.; Eisenreich, W.; Bacher, A.; Huber, R.; Steinbacher, S.; Fischer, M. *Structure* **2002**, *10*, 1371−1381.
(23) Truffault, V.; Coles, M.; Diericks, T.; Abelmann, K.; Eberhardt, S.; Lüttgen, H.; Bacher, A.; Kessler, H. *J. Mol. Biol.* **2001**, *309*, 949−960.
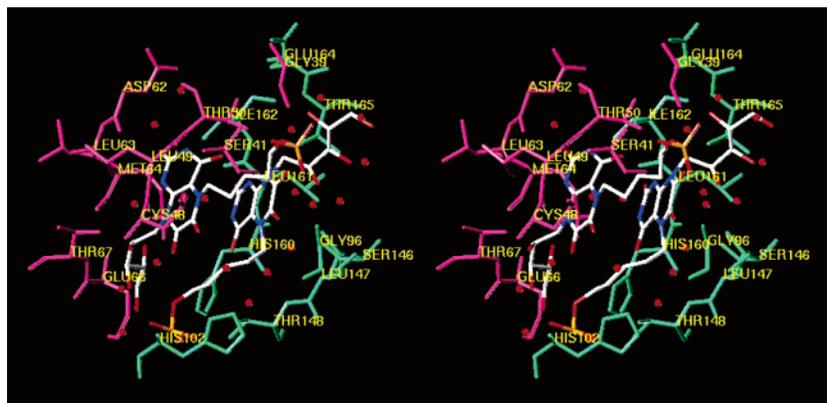
FIGURE 5. Hypothetical model of the binding of two molecules of inhibitor **22** to *E. coli* riboflavin synthase. The C-barrel is magenta and the N-barrel is green. The model is programmed for walleyed viewing.

modeling with lumazine synthase, and the result is displayed in Figure 5. The C-barrel in Figure 5 is colored magenta and the N-barrel is green. The two ligand molecules are stacked with their ribityl side chains pointing in opposite directions, which is consistent with both the known regiochemistry of the riboflavin synthase-catalyzed reaction and the available crystal structures.[3] This means that the two phosphate side chains must also be pointing in opposite directions. Overall, the structure indicates that riboflavin synthase could in fact accommodate two molecules of the inhibitor **22** in the active site.

In conclusion, two alkyl phosphate derivatives of the 6,7-dihydro-6,7-dioxo-8-ribityllumazine system were synthesized and found to be inhibitors of *B. subtilis* and *M. tuberculosis* lumazine synthase as well as *E. coli* riboflavin synthase. The possible binding modes of these compounds were investigated through molecular modeling of complexes formed between compound **22** and both lumazine synthase and riboflavin synthase. Potential antibiotics that inhibit both lumazine synthase and riboflavin synthase would have a potential therapeutic advantage over those that inhibit only one enzyme because microorganisms would have to mutate both enzymes at the same time in order to acquire drug resistance.

Experimental Section

General. Melting points were determined in capillary tubes and are uncorrected. Proton nuclear magnetic resonance spectra (^{1}H NMR) were determined at 300 MHz or at 500 MHz as noted. Silica gel used for column chromatography was 230–400 mesh.

8-(2′,3′,4′,5′-Tetrakis-*t*-butyldimethylsilyl-D-ribityl)-5,6,7,8-tetrahydro-2,4-dimethoxy-6,7-dioxopteridine (16). The nitro compound **15** (4.21 g, 5.32 mmol) was dissolved in methanol (150 mL), and palladium on charcoal (10%, 500 mg) was added. The reaction mixture was hydrogenated at room temperature and 1 atm for 3 days. The catalyst was filtered off, the filtrate was concentrated to remove the solvent completely, and the residue was dried well under vacuum. Triethylamine (2.2 mL, 16 mmol) and dichloromethane (30 mL) were added and the reaction mixture was cooled to 0 °C. A solution of ethyl oxalyl chloride (0.6 mL, 5.32 mmol) in dichloromethane (10 mL) was added dropwise and the mixture was stirred overnight at RT. The reaction mixture was washed with water (2 × 20 mL), dried with anhydrous Na$_2$SO$_4$, filtered, and concentrated under vacuum. The residue was dissolved in absolute ethanol (150 mL) and TEA (20 mL) and heated at

reflux for 72 h. The solvent was removed under reduced pressure, and the residue was purified by flash chromatography (silica gel, 50 g, 230–400 mesh), eluted with hexanes–ethyl acetate (1:1), to furnish pure **16** (1.55 g, 36%) as a foamy solid. ^{1}H NMR (300 MHz, CDCl$_3$) δ 8.52 (s, 1 H), 5.05 (dd, J = 9.9 and 13.15 Hz, 1 H), 4.47 (d, J = 9.9 Hz, 1 H), 4.38 (dd, J = 2.49 and 13.1 Hz, 1 H), 4.12 (s, 3 H), 4.05 (t, J = 2.13 Hz, 1 H), 4.01 (s, 3 H), 3.84 (m, 1 H), 3.72 (m, 1 H), 3.60 (dd, J = 6.03 and 9.64 Hz, 1 H), 0.97 (s, 9 H), 0.90 (s, 9 H), 0.89 (s, 9 H), 0.64 (s, 9 H), 0.19 (s, 3 H), 0.14 (s, 3 H), 0.12 (s, 9 H), 0.07 (s, 3 H), 0.06 (s, 3 H), −0.02 (s, 3 H); IR (KBr) 2954, 2957, 1713, 1603, 1472, 1488, 1378, 1254, 1103, 834 cm^{-1}; EIMS *m/z* 815 (MH$^+$). Anal. Calcd for C$_{37}$H$_{74}$N$_4$O$_4$Si$_8$: C, 54.50; H, 9.15; N, 6.87. Found: C, 54.50; H, 9.16; N, 6.67.

8-(2′,3′,4′,5′-Tetrakis-*t*-butyldimethylsilyl-D-ribityl)-5,6,7,8-tetrahydro-5-(4′-iodobutyl)-2,4-dimethoxy-6,7-di-oxopteridine (17). Compound **16** (300 mg, 0.37 mmol) was dissolved in dry CH$_3$CN (20 mL). Anhydrous K$_2$CO$_3$ (200 mg, 1.45 mmol) and 1,4-diiodobutane (0.24 mL, 1.84 mmol) were added, and the mixture was heated at reflux overnight. The mixture was filtered and the solvent was removed under reduced pressure. The residue was purified by flash chromatography (SiO$_2$, 230–400 mesh) (elution with hexanes–EtOAc 95:5) to afford pure **17** (234 mg, 63.0%) as colorless oil. ^{1}H NMR (300 MHz, CDCl$_3$) δ 5.08 (dd, J = 10.09 and 13.06 Hz, 1 H), 4.42 (d, J = 9.79 Hz, 1 H), 4.34 (t, J = 9.41 Hz, 3 H), 4.09 (s, 3 H), 4.07 (d, J = 13.3 Hz, 1 H), 3.98 (s, 3 H), 3.84 (t, J = 6.48 Hz, 1 H), 3.69 (dd, J = 7.23 and 17.95 Hz, 1 H), 3.58 (dd, J = 6.03 and 10.56 Hz, 1 H), 3.21 (t, J = 6.46 Hz, 2 H), 1.88 (quint, J = 7.21 Hz, 2 H), 1.82 (quint, J = 7.21 Hz, 2 H), 0.94 (s, 9 H), 0.87 (s, 9 H), 0.86 (s, 9 H), 0.62 (s, 9 H), 0.16 (s, 3 H), 0.12 (s, 3 H), 0.09 (s, 6 H), 0.043 (s, 3 H), 0.036 (s, 3 H), −0.055 (s, 3 H), −0.49 (s, 3 H). EIMS *m/z* 997 (MH$^+$). Anal. Calcd for C$_{41}$H$_{81}$-IN$_4$O$_8$Si$_4$: C, 49.37; H, 8.19; N, 5.62. Found: C, 49.21; H, 8.38; N, 5.27.

8-(2′,3′,4′,5′-Tetrakis-*t*-butyldimethylsilyl-D-ribityl)-5,6,7,8-tetrahydro-5-(5′-iodopentyl)-2,4-dimethoxy-6,7-di-oxopteridine (18). Compound **16** (250 mg, 0.31 mmol) was dissolved in dry CH$_3$CN (10 mL). Anhydrous K$_2$CO$_3$ (200 mg, 1.45 mmol) and 1,5-diiodopropane (0.24 mL, 1.53 mmol) were added, and the mixture was heated at reflux overnight. The mixture was filtered and the solvent was removed under reduced pressure. The residue was purified by flash chromatography (SiO$_2$, 230–400 mesh) (elution with hexanes–EtOAc 95:5) to afford pure **18** (211 mg, 68.0%) as a colorless oil. ^{1}H NMR (500 MHz, CDCl$_3$) δ 5.08 (dd, J = 10.14 and 13.01 Hz, 1 H), 4.42 (d, J = 9.78 Hz, 1 H), 4.31 (t, J = 9.41 Hz, 3 H), 4.08 (s, 3 H), 4.05 (d, J = 11.0 Hz, 1 H), 3.98 (s, 3 H), 3.84 (t, J = 5.9 Hz, 1 H), 3.69 (dd, J = 7.23 and 17.95 Hz, 1 H), 3.58 (dd, J = 6.06 and 10.56 Hz, 1 H), 3.18 (t, J = 6.82 Hz, 2 H), 1.85 (quint, J = 7.21 Hz, 2 H), 1.69 (quint, J = 7.21 Hz, 2 H), 1.48 (quint, J = 7.21 Hz, 2 H), 0.94 (s, 9 H), 0.87 (s, 9 H), 0.86 (s,

9 H), 0.62 (s, 9 H), 0.16 (s, 3 H), 0.12 (s, 3 H), 0.09 (s, 6 H), 0.043 (s, 3 H), 0.036 (s, 3 H), −0.057 (s, 3 H), −0.49 (s, 3 H); EIMS *m/z* 1011 (MH⁺). Anal. Calcd for $C_{42}H_{83}IN_4O_8Si_4$: C, 49.88; H, 8.27; N, 5.54. Found: C, 49.79; H, 7.85; N, 5.46.

Dibenzyl 4-[8-(2′,3′,4′,5′-Tetrakis-*t*-butyldimethylsilyl-D-ribityl)-5,6,7,8-tetrahydro-2,4-dimethoxy-6,7-dioxopterid-5-yl]butane 1-Phosphate (19). Compound **17** (0.10 g, 0.10 mmol) and silver dibenzyl phosphate (0.06 g, 0.15 mmol) were heated at reflux in dry CH₃CN (5.0 mL) for 10 h. The solution was then filtered and concentrated under reduced pressure. The resulting oil was purified by silica gel flash chromatography (SiO₂, 230−400 mesh), eluted with hexanes−ethyl acetate (1:1), to furnish the desired compound **19** (0.08 g, 70%) as a colorless oil. ¹H NMR (300 MHz, CDCl₃) δ 7.31 (s, 10 H), 5.07 (dd, *J* = 10.09 and 13.06 Hz, 1 H), 4.99 (m, 4 H), 4.41 (d, *J* = 9.41 Hz, 1 H), 4.33 (d, *J* = 13.15 Hz, 1 H), 4.26 (t, *J* = 6.75 Hz, 2 H), 3.99 (q, *J* = 6.04 Hz, 2 H), 3.98 (s, 3 H), 3.97 (s, 3 H), 3.83 (t, *J* = 6.45 Hz, 1 H), 3.68 (t, *J* = 8.82 Hz, 1 H), 3.57 (dd, *J* = 5.99 and 10.33 Hz, 1 H), 1.67−1.66 (m, 4 H), 0.93 (s, 9 H), 0.87 (s, 9 H), 0.86 (s, 9 H), 0.60 (s, 9 H), 0.15 (s, 3 H), 0.11 (s, 3 H), 0.087 (s, 6 H), 0.038 (s, 3 H), 0.032 (s, 3 H), −0.07 (s, 3 H), −0.52 (s, 3 H); EIMS *m/z* 1147 (MH⁺). Anal. Calcd for $C_{55}H_{95}N_4O_{12}PSi_4$: C, 57.56; H, 8.34; N, 4.88. Found: C, 57.33; H, 8.40; N, 5.28.

Dibenzyl 4-[8-(2′,3′,4′,5′-Tetrakis-*t*-butyldimethylsilyl-D-ribityl)-5,6,7,8-tetrahydro-2,4-dimethoxy-6,7-dioxopterid-5-yl]pentane 1-Phosphate (20). Compound **18** (0.21 g, 0.21 mmol) and silver dibenzyl phosphate (0.12 g, 0.31 mmol) were heated at reflux in dry CH₃CN (10 mL) for 10 h. The solution was then filtered and concentrated under reduced pressure. The resulting oil was purified by silica gel flash chromatography (SiO₂, 230−400 mesh), eluted with hexanes−ethyl acetate (1:1), to furnish the desired compound **20** (0.17 g, 71%) as a colorless oil. ¹H NMR (300 MHz, CDCl₃) δ 7.32 (s, 10 H), 5.08 (dd, *J* = 10.07 and 13.06 Hz, 1 H), 5.01 (m, 4 H), 4.41 (d, *J* = 9.87 Hz, 1 H), 4.33 (d, *J* = 13.17 Hz, 1 H), 4.25 (t, *J* = 7.72 Hz, 2 H), 4.00 (s, 3 H), 3.97 (q, *J* = 6.04 Hz, 2 H), 3.96 (s, 3 H), 3.84 (t, *J* = 5.79 Hz, 1 H), 3.69 (t, *J* = 8.82 Hz, 1 H), 3.58 (dd, *J* = 5.99 and 10.33 Hz, 1 H), 1.65−1.63 (m, 4 H), 1.53 (m, 2 H), 0.94 (s, 9 H), 0.87 (s, 9 H), 0.86 (s, 9 H), 0.61 (s, 9 H), 0.16 (s, 3 H), 0.11 (s, 3 H), 0.092 (s, 6 H), 0.043 (s, 3 H), 0.038 (s, 3 H), −0.061 (s, 3 H), −0.51 (s, 3 H); EIMS *m/z* 1161 (MH⁺). Anal. Calcd for $C_{56}H_{97}N_4O_{12}PSi_4$: C, 57.93; H, 8.36; N, 4.82. Found: C, 57.79; H, 8.06; N, 4.84.

4-(1,5,6,7-Tetrahydro-6,7-dioxo-8-D-ribityllumazin-5-yl)butane 1-Phosphate (21). Compound **19** (82 mg, 0.07 mmol) was dissolved in a solution of [48% HBr−H₂O (2:1)]−MeOH (1:1; 5 mL), and the mixture was stirred at 55−60 °C for 3 h. The solvent was removed in vacuo, the residue was dissolved in MeOH (1 mL), and ethyl ether (5 mL) was added. After 24 h in the refrigerator, the precipitate was filtered out as a white solid, which was dissolved in water (5 mL), decolorized with active charcoal, and filtered. The colorless filtrate was lyophilized to furnish **21** (25 mg, 73%) as a white, highly hygroscopic amorphous solid. ¹H NMR (D₂O) (300 MHz) δ 3.41−4.27 (m, 11 H), 1.45 (m, 4 H); ¹³C NMR (D₂O) (75 MHz) δ 158.7, 156.7, 154.5, 149.9, 137.8, 100.6, 76.4, 73.0, 72.4, 71.6, 70.1, 49.2, 45.8, 26.2, 24.9; ESI-MS (negative ion mode) *m/z* 481 [(M − H⁺)⁻]. Anal. Calcd for $C_{15}H_{23}N_4O_{12}P·0.6H_2O$: C, 36.50; H, 4.91; N, 11.35. Found: C, 36.84; H, 4.71; N, 10.92.

5-(1,5,6,7-Tetrahydro-6,7-dioxo-8-D-ribityllumazin-5-yl)pentane 1-Phosphate (22). This compound was prepared from **20** in 78% yield by the procedure above to afford the product as a white, highly hygroscopic amorphous solid (38 mg, 78%). ¹H NMR (D₂O) (300 MHz) δ 3.64−4.58 (m, 11 H), 1.75 (m, 4 H), 1.52 (m, 2 H); ¹³C NMR (D₂O) (75 MHz) δ 158.7, 156.8, 154.5, 150.0, 137.9, 100.6, 73.0, 72.4, 70.1, 66.6, 62.8, 47.0, 46.1, 29.6, 27.9, 22.4; ESI-MS *m/z* 495 [(M − H⁺)⁻]. Anal. Calcd for $C_{16}H_{25}N_4O_{12}P·0.5H_2O$: C, 37.99; H, 5.14; N, 11.08. Found: C, 37.98; H, 4.85; N, 10.73.

Molecular Modeling on Lumazine Synthase. By use of Sybyl (Tripos, Inc., version 7.0, 2004), the X-ray crystal structure of the complex of 5-nitro-6-ribitylamino-2,4-(1*H*,3*H*)-pyrimidinedione (**25**) and the lumazine synthase of *B. subtilis* (1RVV)[19] was clipped to include information within a 15 Å-radius of one of the 60 equivalent ligand molecules. The residues that were clipped in this cut complex were capped with either neutral amino or carboxyl groups. The structure of the inhibitor **22** was overlapped with the structure of 5-nitro-6-ribitylamino-2,4-(1*H*,3*H*)pyrimidinedione (**25**), which was then deleted. Hydrogen atoms were added to the complex. MMFF94 charges were loaded, and the energy of the complex was minimized by the Powell method to a termination gradient of 0.05 kcal/mol while the MMFF94s force field was employed. During the minimization of the complex, inhibitor **22** and a 6 Å sphere surrounding it were allowed to remain flexible, while the remaining portion of the complex was held rigid by use of the aggregate function. Figure 3 was constructed by displaying the amino acid residues of the enzyme that are involved in hydrogen bonding with the inhibitor **22**.

Molecular Modeling on Riboflavin Synthase. By use of Sybyl (Tripos, Inc., version 7.0, 2004), the X-ray crystal structure of *E. coli* riboflavin synthase (1I8D) was downloaded and two molecules of the ligand **22** were docked and oriented as suggested by the published model of the binding of two molecules of the substrate **1** in the active site,[21] as well as by the structure of **22** bound to *S. pombe* riboflavin synthase.[22] The C- and N-terminal groups were changed to neutral carboxylic acid and amino groups, and hydrogens were added to the protein structure and to the oxygens of the water molecules. MMFF94 charges were loaded, and the energy of a 6 Å-radius spherical subset including and surrounding the two ligand molecules was minimized by the Powell method to a termination gradient of 0.05 kcal/mol while the MMFF94s force field was employed. During energy minimization, the remaining protein structure was held rigid by use of the aggregate function. Figure 5 was constructed by displaying the amino acid residues in the C- and N-barrels surrounding the two ligand molecules.

Lumazine Synthase Assay.[24] The experiments with *B. subtilis* lumazine synthase were performed as follows. Reaction mixtures contained 100 mM potassium phosphate, pH 7.0, 5 mM ethylenediaminetetraacetic acid (EDTA), 5 mM dithiothreitol, inhibitor (0−500 μM), 150 μM L-3,4-dihydroxy-2-butanone 4-phosphate (**2**), and *B. subtilis* lumazine synthase (7 μg, specific activity 12.8 μmol mg⁻¹ h⁻¹) in a total volume of 1000 μL. The solution was incubated at 37 °C, and the reaction was started by the addition of a small volume (20 μL) of 5-amino-6-ribitylamino-2,4(1*H*,3*H*)-pyrimidinedione (**1**) to a final concentration of 5−100 μM. The experiments with *M. tuberculosis* lumazine synthase were conducted as follows. Reaction mixtures contained 50 mM Tris HCl, pH 7.0, 100 mM NaCl, 5 mM EDTA, 5 mM dithiothreitol, 150 μM L-3,4-dihydroxy-2-butanone 4-phosphate (**2**), inhibitor (0−500 μM), and *M. tuberculosis* enzyme (12.5 μg, specific activity 4.3 μmol mg⁻¹ h⁻¹) in a total volume of 1000 μL. The mixtures were incubated at 37 °C, and the reaction was started by the addition of a small volume (20 μL) of substrate **1** to a final concentration of 20−400 μM. The formation of 6,7-dimethyl-8-ribityllumazine (**3**) was measured online with a computer-controlled photometer at 408 nm ($\epsilon_{lumazine}$ = 10 200 M⁻¹cm⁻¹). The velocity−substrate data were fitted for all inhibitor concentrations with a nonlinear regression method by use of the program DynaFit.[25] Different inhibition models were considered for the calculation. K_i and K_{is} values ± standard deviations were obtained from the fit under consideration of the most likely inhibition model.

Riboflavin Synthase Assay.[26] Reaction mixtures contained buffer (100 mM potassium phosphate, pH 7.0, 10 mM EDTA, and 10 mM sodium sulfite), inhibitor (0−300 μM), and

(24) Kis, K.; Bacher, A. *J. Biol. Chem.* **1995**, *270*, 16788−16795.
(25) Kuzmic, P. *Anal. Biochem.* **1996**, *237*, 260−273.
(26) Eberhardt, S.; Richter, G.; Gimbel, W.; Werner, T.; Bacher, A. *Eur. J. Biochem.* **1996**, *242*, 712−718.

riboflavin synthase (1.2 μg, specific activity 45 μmol mg^{-1} h^{-1}). After preincubation, the reactions were started by the addition of various amounts of 6,7-dimethyl-8-ribityllumazine (**3**) (2.5–200 μM) to a total volume of 1000 μL. The formation of riboflavin (**4**) was measured online with a computer-controlled photometer at 470 nm ($\epsilon_{\text{riboflavin}}$ = 9600 M^{-1} cm^{-1}). The evaluation of data sets was performed in the same manner as described above.

JO051332V